Static stability

(i)   The concept of stability

The concept of (local) stability is an important one in meteorology. In general, the word stability is used to indicate a condition of equilibrium. A system is stable if it resists changes, like a ball in a depression. No matter in which direction the ball is moved over a small distance, when released it will roll back into the centre of the depression, and it will oscillate back and forth, until it eventually stalls. A ball on a hill, however, is unstably located. To some extent, a parcel of air behaves exactly like this ball.

Certain processes act to make the atmosphere unstable; then the atmosphere reacts dynamically and exchanges potential energy into kinetic energy, in order to restore equilibrium. For instance, the development and evolution of extratropical fronts is believed to be no more than an atmospheric response to a destabilizing process; this process is essentially the atmospheric heating over the equatorial region and the cooling over the poles. Here, we are only concerned with static stability, i.e. no pre-existing motion is required, unlike other types of atmospheric instability, like baroclinic or symmetric instability. The restoring atmospheric motion in a statically stable atmosphere is strictly vertical. When the atmosphere is statically unstable, then any vertical departure leads to buoyancy. This buoyancy leads to vertical accelerations away from the point of origin. In the context of this chapter, stability is used interchangeably with static stability.

The most general application of stability is in synoptic-scale weather forecasting; stability concepts are used, for instance, in the identification of

- <u>unstable</u> conditions suitable for the formation of convective clouds, from fair weather cumuli to severe thunderstorms;

- a variety of stable conditions:

    o warm or cold fronts aloft, recognized by an elevated inversion, often capped by a saturated layer of air, indicating uplift, unlike a subsidence inversion, which is;

    o subsidence inversions, capped by a dry layer (unlike frontal inversions), which indicates descent of tropospheric air; they are associated with low-level highs or ridges (see further);

    o turbulence inversions which develop as a result of frictional mixing, typically close to the surface (see further);

    o radiation inversions which form on clear nights when the ground cools more rapidly than the air above. In urban locations these conditions can lead to the trapping of pollutants emitted by industrial sources and motor vehicles, thereby affecting the quality of the air.

Therefore, a knowledge of the concepts of stability and how the thermal structure of the atmosphere changes in space and time is needed to understand changing weather conditions.

(ii)   The parcel technique

(a)   Stable, neutral and unstable

The stability of any part of the atmosphere can be determined from its Environmental lapse rate (ELR) and, in some conditions, its dewpoint lapse rate (DLR). Perhaps the best way to explain how static stability can be determined is to disturb a dry (unsaturated) parcel of air in the hypothetical case of **Fig 1**.

Take a parcel of air at point P and lift it over a short distance. Assume that the parcel does not mix with the surrounding air and remains thy, so its vertical movement will be dry-adiabatic, i.e. upon rising its temperature will decrease at a rate of l°C/100 m (the DALR). It will, on Fig 1a, follow the DALR. Since the potential temperature (9) of a dry air parcel is conserved, a parcel will follow a vertical line on a θ-z plot (Fig 1b). It is obvious, then, that if it is lifted, it will be colder than the environment (ELR) (Fig 1a). It follows from the equation of state (at constant pressure) that it must be denser, and hence heavier than the environment. Since the environment is in a state of hydrostatic equilibrium, the parcel must have a downward gravity force greater than the upward pressure gradient

force. In other words, the parcel is negatively buoyant, and it sinks back to the point P. This displacement is illustrated in Figs. 9a and 9b.

A similar argument will show that if it is initially forced downward it will be warmer than the surroundings, and will experience an upward force and also will return to its initial position. Clearly, the ELR is stable in this case. In other words, a layer of air is said to be in local stable equilibrium if, after any displacement of a parcel from its initial position, it experiences a force which returns it to that point. Compare this to the situation depicted in Fig 1c; in this case, the ELR is parallel to the DALR (that is a vertical line on a θ -z plot). An air parcel, whether lifted or subsided, will always be at the same temperature as the environment. The atmospheric profile is neutral in this case.

Finally, in Fig 1d, the ELR tilts to the left of the vertical on a θ -z plot. A parcel, when lifted from P, will be warmer than the environment, and it will continue to rise spontaneously. If the parcel were forced downward, it would have been colder than the environment, and it would have fallen further. This ELR is locally unstable.

Note that in a stable atmosphere, a perturbed parcel does not simply return to its original position. Instead, once perturbed, it will oscillate vertically around its original position, with a frequency (or oscillation rate) called the Brunt-Väisällä frequency (after the names of a British and a Finnish meteorologist). The oscillation will only be damped by friction and mixing.
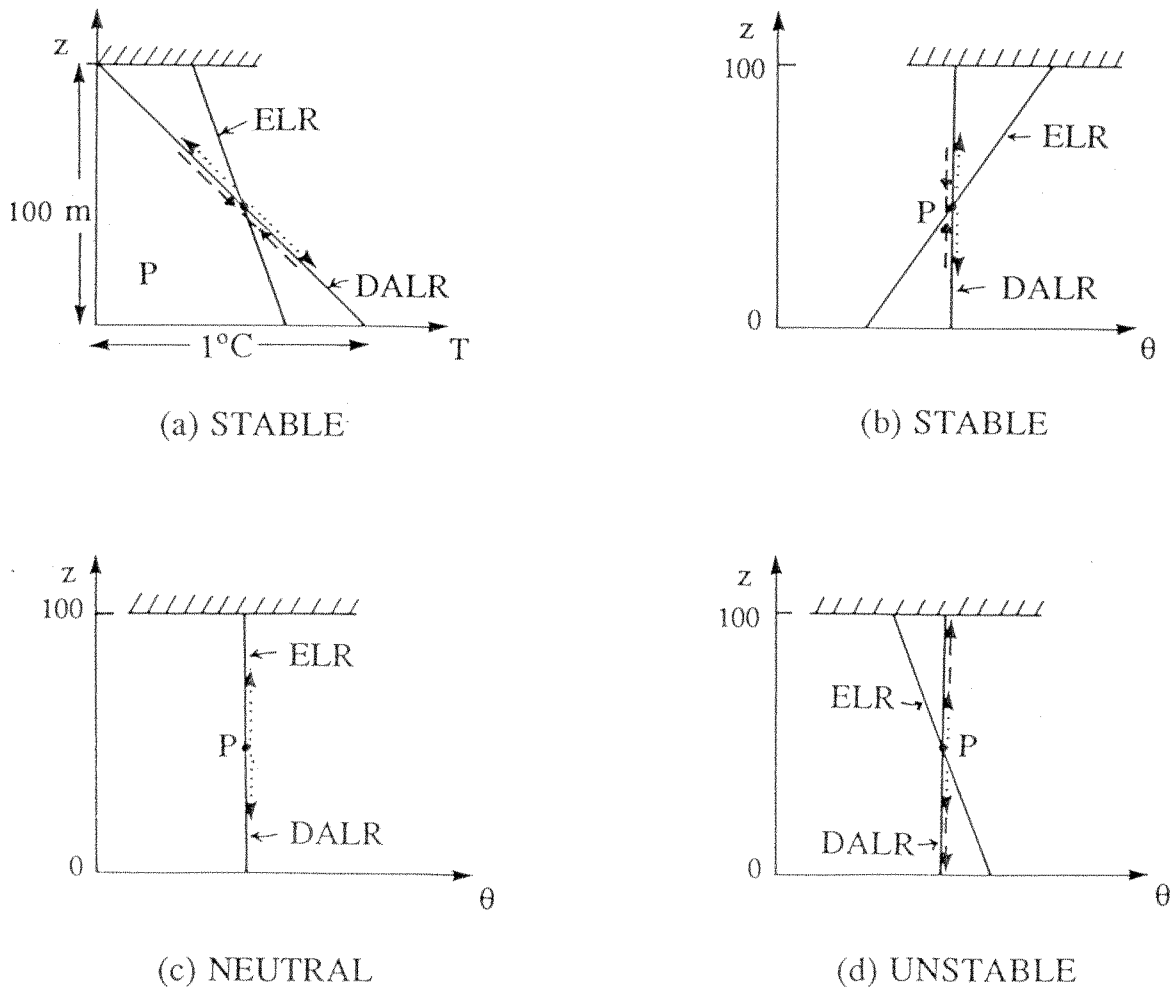
Fig 1. Local atmospheric stability for a dry parcel. (a) stable ELR on a T-z diagram; (b) ibidem, plotted on a θ-z diagram; (c) a neutral ELR; (d) an unstable ELR. The point of reference is P. The dotted arrow traces the initial displacement of a parcel. The dashed arrow shows the parcel's response.

The movement of an air parcel can be compared with that of a ball on a non-level surface. A ball, pushed slightly sideways out of the centre of a depression, will converge in a damped oscillation towards the centre. If there were no friction, the ball would never stall. The frequency of the oscillation depends on the shape of the depression; deeper depressions have a higher frequency. Similarly, the oscillation frequency of an air parcel depends on atmospheric stability; the Brunt-Vaisalla frequency in an inversion is larger than that in a marginally stable layer.

The theory is as follows: assume that the environment is in hydrostatic balance,

$$\frac{d\overline{p}}{dz} = -\overline{\rho}g$$

where the over-bars refer to the basic state, which is a function of height z only. A parcel of air that is displaced vertically assumes the environmental pressure $\overline{p}$ instantaneously (see footnote 5). It will conserve its potential temperature, which is $\overline{\theta}$ at height z, while the environment has a variable lapse rate $\frac{d\overline{\theta}}{dz}$. Then, at a finite displacement δz, the parcel has a potential temperature $\overline{\theta}$, while the environment has a potential temperature $\overline{\theta} + \frac{d\overline{\theta}}{dz}\delta z$. Let δθ be the difference in potential temperatures between parcel and environment. Then $\delta\theta = -\frac{d\overline{\theta}}{dz}\delta z$. From the definition of potential temperature, the ideal gas law, and the equation of Mayer ($c_p = c_v + R_d$), it follows that:

$$\frac{d\theta}{\theta} = -\frac{d\rho}{\rho} + \frac{c_v}{c_p}\frac{dp}{p} \tag{1}$$

So the difference in potential temperatures between parcel and environment at height z + δz is:

$$\delta\theta = -\overline{\theta}\frac{\delta\rho}{\overline{\rho}} \tag{2}$$

since the pressure adjusts instantaneously. δρ is the difference in density between parcel and environment. It is assumed that $\delta\rho << \overline{\rho}$. Both $-g\frac{\delta\rho}{\overline{\rho}}$ and $g\frac{\delta\theta}{\theta}$ are expressions of the buoyancy of an air parcel. The parcel's density is $\rho = \overline{\rho} + \delta\rho$. The vertical equation of motion is:

$$\frac{dw}{dt} = \frac{d^2\delta z}{dt^2} = -\frac{1}{\rho}\frac{dp}{dz} - g = -\frac{1}{\overline{\rho}}\frac{dp}{dz} - g + \frac{\delta\rho}{\overline{\rho}^2}\frac{dp}{dz} \tag{3a}$$

since the pressure perturbation is zero [hint: use: $\frac{1}{\overline{\rho}+\delta\rho} = \frac{1}{\overline{\rho}}\frac{1}{(1+\frac{\delta\rho}{\overline{\rho}})} \cong \frac{1}{\overline{\rho}}(1-\frac{\delta\rho}{\overline{\rho}})$]. Now use the hydrostatic equation to obtain:

$$\frac{d^2\delta z}{dt^2} = -g\frac{\delta\rho}{\overline{\rho}} = g\frac{\delta\theta}{\overline{\theta}} = -\frac{g}{\overline{\theta}}\frac{d\overline{\theta}}{dz}\delta z \tag{3b}$$

So

$$y'' + N^2 y = 0 \tag{4}$$

1/20/2014

where $y = \delta z$ and y'' is its second derivative with time t, and

$$N^2 = \frac{g}{\bar{\theta}} \frac{d\bar{\theta}}{dz}$$

is the square of the Brunt-Vaisalla frequency. The general solution of (34) is $y = Ae^{(iNt)}$ where A is a constant. Clearly, when $N^2 < 0$, the solution increases exponentially with height, i.e. the atmosphere is unstable. The criterion for static instability then is:

$$\boxed{\frac{d\bar{\theta}}{dz} < 0}$$ (5)

Usually, $N^2 > 0$, in which case the solution of (4) is oscillatory, and the oscillation has a period (called buoyancy period) of $\frac{2\pi}{N}$.
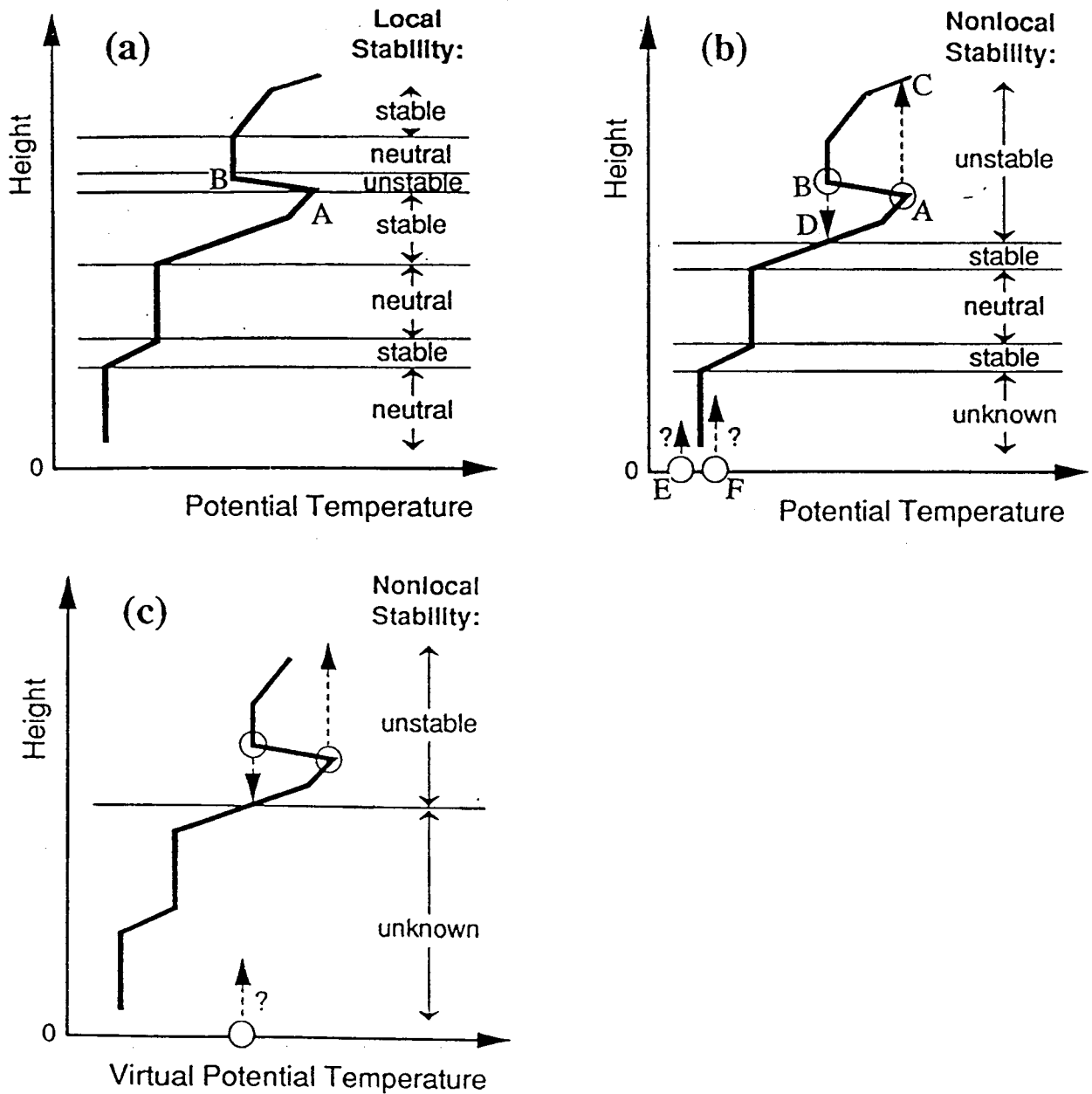
(b)   Local and non-local stability

To carry on with the analogy, it is clear that a ball in a depression is stable. So far, we have assumed that any perturbation is infinitesimal, i.e. that the displacements are small. In other words, we have considered *local stability*. However, if a parcel were originally positioned on a high hill above the depression, it would, when released, roll down (a hill corresponds to an unstable ELR), roll through the depression and across the adjacent hill, and never return (**Fig 2**). Therefore, while a depression is locally stable (by definition), it is in the case of Fig 2 non-locally unstable. Non-local stability depends on the surroundings. Therefore, whenever in the real troposphere atmospheric stability is evaluated, the entire profile from ground to tropopause should be known. It is for this reason also that, to eliminate non-local effects, the ELR's analysed in Fig 1 are confined at the top and the bottom.

locally unstable
non-locally unstable

locally unstable
non-locally unstable

Fig 2. Local vs non-local instability.

To further illustrate the difference between local and non-local stability, consider **Fig 3**. From Figs 9b and 9d it is clear that when the ELR tilts to the right with height, it is (locally) stable, and that when it tilts to the left, it is (locally) unstable. A vertical ELR is (locally) neutral (Fig 1c). This can be verified in Fig 3a, which shows an arbitrary, unbounded ELR on a θ-z plot. The non-local stability distribution is quite different (Fig 3b). The locally unstable layer (Fig 3a) is non-locally a much thicker layer, mainly because the amount of local instability is so large (compare to a ball on a steep hill). The non-locally unstable zone extends from the warm peak (A) upwards to where it intersects with the ELR (C), and from the coldest part of the locally unstable zone (B) downwards, again to the intersection with the ELR (at D). The latter can be understood by pushing a parcel downwards from B; it will be colder than the environment and continue downwards (unstable) until it reaches D. Beyond D, it would be warmer than the environment, and it would ascend, so its stalls at D. Only the locally stable zone below D is non-locally stable. In terms of non-local stability, the neutral and stable areas are smaller (Fig 3 b), and they may disappear in the vicinity of a strong locally unstable layer. Because in this case the ELR is unbounded, the non-local stability is theoretically entirely unkown. Practically, the potential temperature at the surface is estimated in Fig 3b between E and F, so only the non-local stability of the lowest layer is unknown. If the potential temperature at the surface was

less certain, the non-local stability of a larger section would be unknown (Fig 3c). In what follows, we will focus on local and non-local stability in a confined domain with known boundaries.

Fig 3. Illustration of local vs non-local stability. The circles represent air parcels, and dashed lines show buoyant parcel movement. (a) local stability analysis; (b) non-local stability analysis, with a fair guess of surface temperature; (c) ibidem, but surface temperature less-known. (from Stull 1991)

(c)   Absolute and conditional stability

Consider the diagram in Fig 4 to be a very much simplified version of an aerological diagram. The lapse rates in cases I, II and III are confined at the top and the bottom, in order to focus on local stability and ignore non-local effects. It can be seen that three possible cases (I,II, and III) of an actual ELR have been plotted onto the diagram: the SALR and DALR through a representative point P on the temperature profile have also been included.

Case I: absolute stability: - In **Fig 5**, if the parcel was initially saturated, so that it would follow the moist adiabat when moved upward, it would still be colder than its surroundings (or warmer if moved downward) and thus would also be restored to its initial position. Again we have stability. The situation (or atmosphere) wherein either a dry or a saturated parcel is in a stable state is called an <u>absolutely stable</u> condition (or atmosphere).
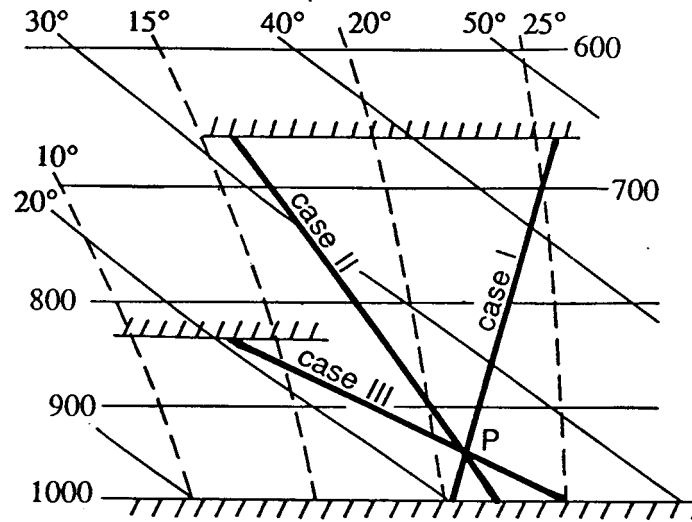

Fig 4. Case I is absolutely stable, case II conditionally stable, and case III absolutely unstable.
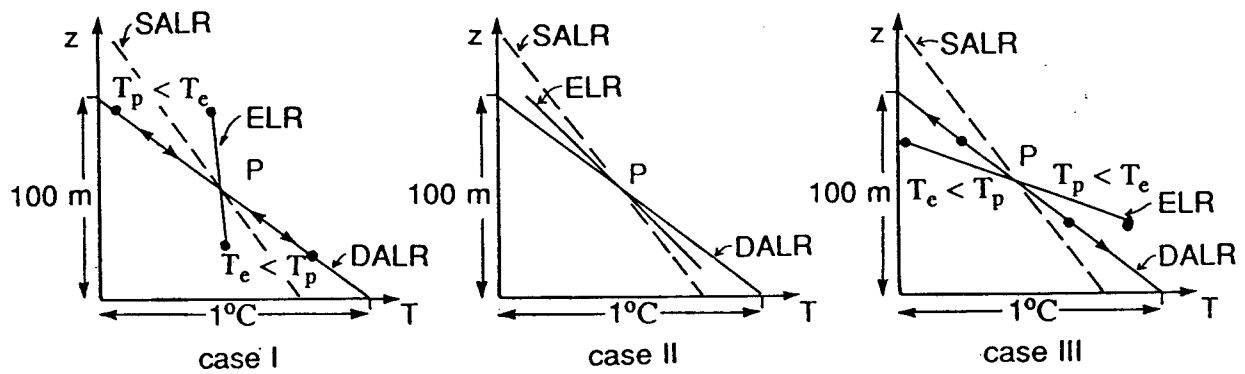

Fig 5. Three cases of stability (Fig 4) shown on a T-z diagram. The reference point is marked as P. After displacement, the parcel and ambient temperatures are denoted as T_p and T_e, respectively.

Case II: conditional instability: - using the arguments above it can be seen that if the parcel is dry, the atmosphere in case II will be stable. On the other hand, if the parcel was saturated, then lifting (moving it along the moist-adiabat) would make it warmer than the environment. It is therefore less dense and lighter, and must experience an upward force. It will move away from the point P for as long as it remains warmer than the air around it. Such a condition is unstable. In other words, instability of a layer is that state wherein, if a parcel is displaced even slightly from its original position, it will continue to move away. The arguments above will also show that a saturated parcel will continue to sink downward if depressed from point P, as long as moisture is available for evaporation upon warming. Since the stability depends on whether or not the parcel is dry, this situation is referred to as <u>conditionally unstable</u>. That is, the layer is stable when dry, unstable when saturated.

• *Case III: <u>absolute instability</u>*: - in this case, an analysis based on the procedures above will show that regardless of whether the parcel is dry or moist, it will always move away from P if it is displaced slightly, as shown in Fig 5. The environment is said to be in an <u>absolutely unstable</u> state.

This discussion is based on the diagram of the three possible general positions of the actual ELR and their relation to the DALR ISALR. The technique discussed above should enable you to determine the stability for any ELR, if you know the degree of saturation of the parcel. The latter can be determined by means of the DLR. Obviously,when T = T_d, then the parcel is saturated. Else, you know that a rising parcel becomes saturated when r_s is reached. The mixing ratio r is conservative for uplift, so the parcel is saturated when the mixing ratio at the dewpoint T_d is reached. Therefore, a parcel will ascent dry-adiabatically until it intersects with the saturation mixing ratio line through T_d at the reference level. From there on, it behaves like a saturated parcel.

The term neutral stability is used for all marginal cases: for instance, if the ELR coincides more or less with the DALR, the ELR is (dry) neutral. If the air is saturated and the ELR is very close to the SALR, then the ELR is moist neutral.

(iii)   The slope technique

Now that you familiarized yourself with the parcel technique to analyze stability, you may know that there is another technique which is much quicker but not as intuitive. Referring to Fig 4, it can be seen that if the ELR, when plotted on the aerological diagram, is inclined to the left of DALR, it corresponds to unstable conditions. By the same token, the conditionally unstable ELR has a slope which lies between the DALR and the SALR. And an ELR which is tilted to the right of SALR is stable. An isothermal ELR, for instance, is quite stable. An inversion is even more stable.

The lapse rate is merely change in temperature change in height and is positive when temperature <u>decreases</u> upward. Thus the lapse rate of profile I is less than the lapse-rate of II, which in turn is less than that of III. Following the argument it can be seen that:

- lapse rate I is less than both the dry and moist adiabatic lapse rates,

- lapse rate II is between the dry and moist adiabatic lapse rates,

- lapse rate III is greater than both the dry and moist adiabatic lapse rates.

Formalized verbally: there is

- absolute stability when the ELR is less than the SALR ($\gamma < \Gamma_s$);

- conditional instability when the ELR is greater than the SALR, less than the DALR ($\Gamma_s < \gamma < \Gamma_d$);

- absolute instability when the ELR is greater than the DALR ($\gamma > \Gamma_d$).

The DALR is symbolized by Γ_d, the SALR by Γ_s, and the ELR by γ.

(iv)   Conditional instability

Conditional instability can easily be determined from the slope of the ELR, as discussed previously. In the absence of an aerological diagram (e.g. in a NWP model), conditional instability can be determined via a simple criterion:

$$\boxed{\frac{d\bar{\theta}_e^{*}}{dz} < 0} \tag{6}$$

This criterion is similar to the criterion for absolute instability (5), but it involves the saturated equivalent potential temperature θ_e^*. This is not surprising, since both conditional instability and θ_e^* ignore the actual availability of water vapor. To prove (6), we follow an argument similar to the one that led to (5). But now $\delta\theta$, the difference in potential temperatures between the parcel and the environment ($\theta_{parcel} - \theta_{environment}$), after lifting over a displacement δz, is

$$\delta\theta = (\bar{\theta} + \delta\theta_{cond}) - (\bar{\theta} + \frac{d\bar{\theta}}{dz}\delta z) = \delta\theta_{cond} - \frac{d\bar{\theta}}{dz}\delta z \qquad (7)$$

where $\delta\theta_{cond}$ represents the condensational heating of the parcel (if it were saturated). If the only diabatic heat source is evaporation/condensation, then the first law of thermodynamics is:

$$c_p dT_v - \alpha dp = -Ldq$$

where L is the latent heat of vaporization, and q the specific humidity, and $\alpha=1/\rho$. We use the ideal gas law to transform this to:

$$\frac{dT_v}{T_v} - \frac{R}{c_p}\frac{dp}{p} = -\frac{L}{c_p T_v}dq$$

or

$$\frac{d\theta}{\theta} = -\frac{L}{c_p T_v}dq$$

From this it follows that $\delta\theta_{cond}$ in (7) can be approximated as,

$$\delta\theta_{cond} = -\bar{\theta}\frac{d}{dz}(\frac{Lq_s}{c_p T_v})\delta z$$

Therefore the buoyancy of the parcel of air, $g\dfrac{\delta\theta}{\bar{\theta}}$, is, with (7):

$$g\frac{\delta\theta}{\bar{\theta}} = -g\left\{\frac{1}{\bar{\theta}}\frac{d\bar{\theta}}{dz} + \frac{d}{dz}(\frac{Lq_s}{c_p T_v})\right\}\delta z = -g\frac{d}{dz}\left(\ln\bar{\theta} + \frac{Lq_s}{c_p T_v}\right)\delta z = -g\frac{d\ln\bar{\theta}_e^*}{dz}\delta z \qquad (8)$$

following the definition of θ_e^*,

$$\theta_e^* \equiv \theta.e^{(\frac{Lq_s}{c_p T_v})}$$

Clearly, from (8) a modified Brunt-Vaisalla frequency can be derived, following the steps in (3).This *saturated Brunt-Vaisalla frequency* N_s is:

$$N_s^2 = g\frac{d\ln\theta_e^*}{dz} \qquad (9)$$

(9) shows that a (necessary and sufficient) condition for conditional instability ($N_s^2<0$) is that the ambient θ_e^* decreases with height, i.e. criterion (6). This criterion should be compared to the one for absolute instability (5) and for potential instability (see Section *vii*, below). The saturated Brunt-Vaisalla frequency N_s is the frequency of a (conditionally) stable parcel that is kept moist during the oscillation. Under the same environmental conditions, $N>N_s$ or the period for a dry parcel is shorter than the period for a moist parcel, in a stable environment. This is a factor in the explanation of the asymmetry of mountain lee waves and of downslope wind storms in the lee of mountains: the descent (dry) is faster then the ascent (moist).

Typical profiles of θ, θ_e, and θ_e^* in the vicinity of tropical deep convection are shown in **Fig 6**. Clearly, the lower troposphere is absolutely stable at all levels, but least so in the PBL. The lower half of the atmosphere (1000- 500 hPa) is conditionally unstable. However, this does not imply that convection spontaneously develops. The release of conditional instability requires saturation at some level. The lowest third of the atmosphere (1000-666 hPa) is potentially unstable, as will be discussed in Section *vii* below.

Conditional instability is by no means uncommon. The reason why the instability rarely materializes into convection is that typically the atmosphere is fairly dry, even in the PBL. It is not easy to determine, in a conditionally unstable situation, how likely it is that unstable motions (convection) will develop. This depends on the details of the ELR and the DLR
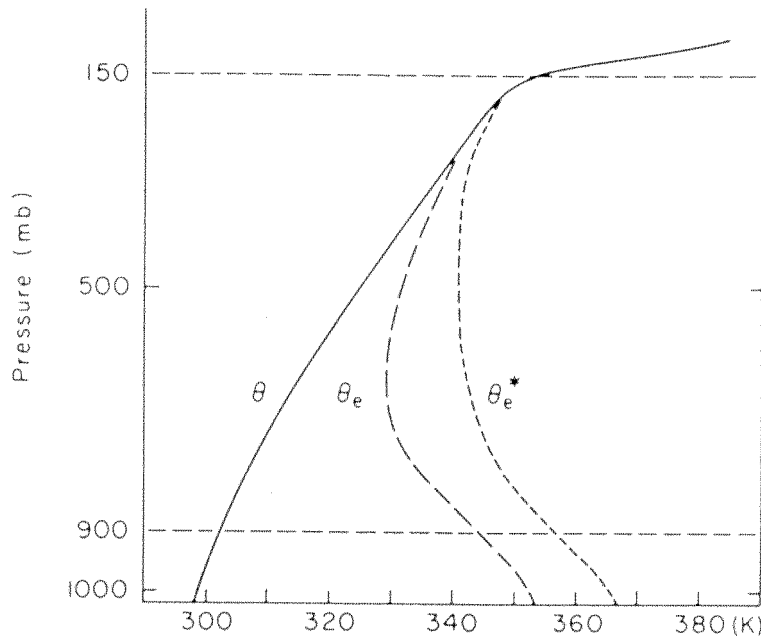

Fig 6. Typical sounding of θ, θ_e, and θ_e* in the intertropical convergence zone. (from Holton '92).

(v)   Convective available potential energy (CAPE), and convective inhibition (CIN)

The only way to assess the likelihood of convection is by means of the parcel method. In **Fig 7** the parcel will certainly be buoyant for a considerable height; for example, at the level of maximum buoyancy, the parcel temperature T is larger the ELR temperature T_e. However, unless the parcel is saturated, it will follow at least a short section of dry adiabat before it ascends moist adiabatically. Notice that at the LCL, the parcel is colder than the environment (point D is colder than B, i.e. $T_D < T_B$). Therefore, even in the least stable situation of conditional instability, the parcel will be negatively buoyant when it penetrates through the first layers of air. So the parcel will need external energy to rise. The negative buoyancy is often referred to as *convective inhibition* CIN (Fig 7). The amount of energy required to penetrate to the *level of free convection* (LFC, Fig 7) is proportional to the area described by the ELR (line ABC) and the parcel trajectory (line ADC).

The source of this energy can be of two types:

• **sustained uplift**: - all the energy (CIN) is derived from the airflow. For instance: sustained lifting over a mountain or a frontal surface, the large scale lifting by upper level divergence due to changes in wind speed/direction aloft, or a frontogenetic circulation. Rapid updrafts occur within the convective PBL, in thermals, but these thermals are short-lived, and by themselves they will not penetrate the lid. The importance of sustained uplift is NOT to force the air through the CIN region (area ABCDA), but rather, to alter the T and T_d lines (see potential instability, thereby reducing the CIN, eventually allowing a lucky thermal to break through. The sustained mesoscale uplift itself is not the result of buoyancy, but rather is due to forced convergence (e.g. over a mountain) or to some dynamical response to a larger-scale imbalance.
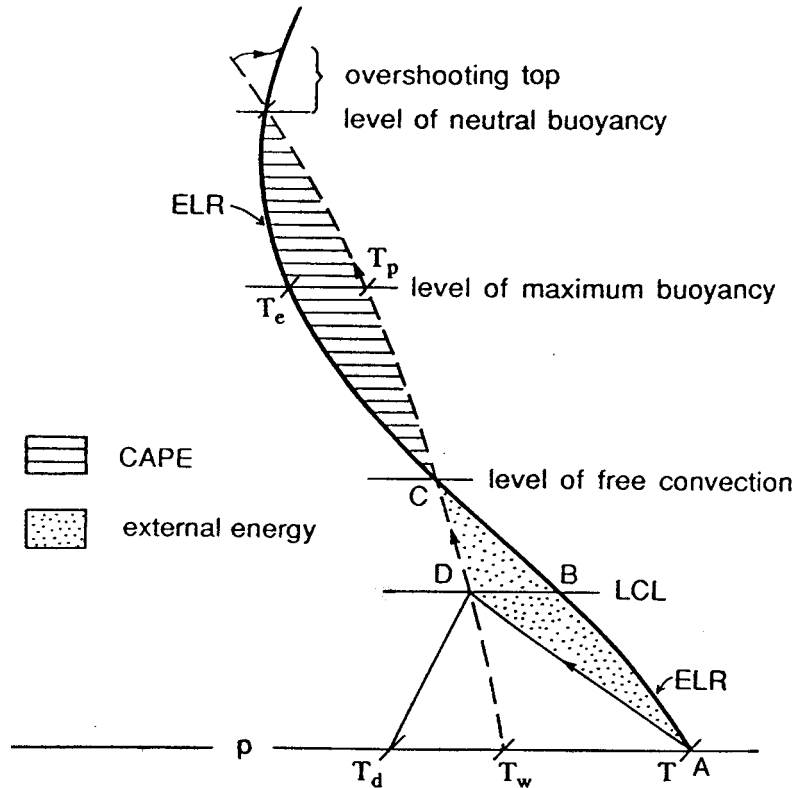
Fig 7. Parcel trajectory (thin line) vs the ELR (bold line). The parcel is shown as a solid line along a dry adiabat and a dashed line along a moist adiabat. The "external"energy is commonly known as CIN (convective inhibition).

• **thermal forcing**: - the size of the area ABCDA can be reduced by altering the temperature and/or dewpoint at the lower boundary. Thermal forcing also increases the area of positive buoyancy above the level of free convection. In other words, thermal forcing increases the moist static energy of the lower ELR, and increases the amount of energy that can be released by convection. Changes in moist static energy can be due to:

- direct (sensible) healing (**Fig 8a**), which occurs during the daytime over land; this effect raises the LCL (LCL_2 is higher than LCL_1)

- latent heating, i.e. the moistening of the lower layer (**Fig 8b**), which typically occurs by advection; this effect lowers the LCL.

The occurrence of anomalously hot and moist air is usually a reliable precursor of severe storms. However thermal forcing itself is often not sufficient. It usually only reduces the amount of sustained uplift required. It is rarely clear what exactly triggers the release of the instability. Notice also that the analysis presented here assumes that any thunderstorms resulting from conditional instability are relatively small; thunderstorm complexes (*mesoscale convective systems*) may impact directly on what is referred to as the 'environmental' lapse rate.

The ceiling of the convection is given as a first approximation by the *level of neutral buoyancy* LNB (Fig 7b). Thunderstorms occur in conditionally unstable situations. The vigor of a thunderstorm is proportional to the amount of potential energy it releases. Per unit mass, a parcel of depth dz has an amount of potential energy dP equal to its (upward) buoyancy force times vertical displacement dz:

$$dP = \frac{\delta\theta}{\overline{\theta}} g dz \qquad (10)$$

or, with the aid of hydrostatic balance and the ideal gas law:

$$dP = -R\delta T_v d \ln p \tag{11}$$

where δT_v is the virtual temperature difference between the parcel and the ELR.
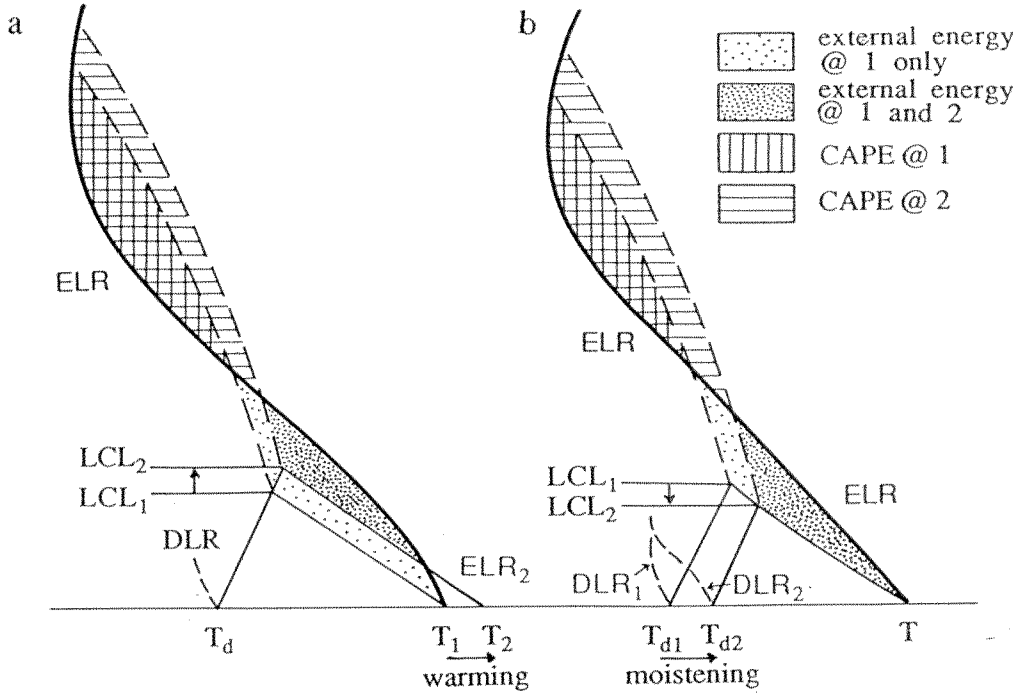
Fig 8. The effect of the increase of (a) temperature and (b) dewpoint on the LCL and the amount of CAPE and CIN.

The integral of dP, from the level of free convection to the level of neutral buoyancy, is referred to as the convective available potential energy (CAPE) P,

$$P = -R \int_{LFC}^{LNB} \delta T_v d \ln p \qquad^1 \tag{12}$$

which can visually be estimated by the shaded area in Fig 7, on a tephigram. A box is shown in the lower left corner of your tephigram: the area of this box corresponds with 300 J/kg. The integral (12) can be expressed in terms of finite differences, with a pressure increment of 10 hPa for instance. The CAPE equals the maximum amount of (potential) energy that can be released by a convective cloud (of unit mass). The larger the area (i.e., the larger the CAPE) and the smaller the area of CIN (external energy), the more likely the occurrence of a severe storm is. Therefore, the area of CAPE is often referred to as the positive area, whereas the area of CIN is called the negative area. CIN is calculated in the same way as (12), but the integral bounds are surface (or mixed-layer top) to LFC. Part of the CAPE, once released, is converted into the kinetic energy of the updrafts. In turn, this energy is lost by entrainment and by the penetration of an overshooting top into the stable environment above the LNB (Fig 7).

• Estimating CAPE (or CIN) from sounding data (without calculating parcel temperature).

According to parcel theory, the parcel temperature equals the surface wet-bulb potential temperature $\theta_{w,sfc}$ at all levels above the LCL, in other words, the parcel follows a moist adiabat from the LCL up. At any level i, the moist adiabat through the ambient air temperature T_i can be expressed as $\theta_{w,i}^*$, the saturated wet-bulb potential

---

[1] Note that P>0 since, in pressure units, LFC>LNB.

temperature. Note that θ_w^* relates to θ_w in the same way as θ_e^* relates to θ_e , i.e., it is assumed that the air is saturated. Then at any level i between the LFC and the LNB, $\delta T_i = \theta_{w,sfc} - \theta_{w,i}^*$, and thus CAPE can be estimated from sounding data as follows:

$$P = R\sum_i (\theta_{w,sfc} - \theta_{w,i}^*)\frac{\Delta p_i}{p_i} \quad \text{for all levels (i) where } \theta_{w,sfc} > \theta_{w,i}^* \tag{13}$$

The term $\dfrac{\Delta p_i}{p_i} = 2\dfrac{p_i - p_{i+1}}{p_i + p_{i+1}}$ in finite differences. The advantage of this approach is that one can readily redefine the parcel's moist adiabat. Sometimes the lowest 50-100 hPa are mixed first (constant θ and q). In terms of (13), the 'mixed-layer' CAPE is obtained by replacing $\theta_{w,sfc}$ by the average wet-bulb potential temperature $\dfrac{1}{N}\sum_{ML}\theta_w$ over the mixed-layer (ML) depth.
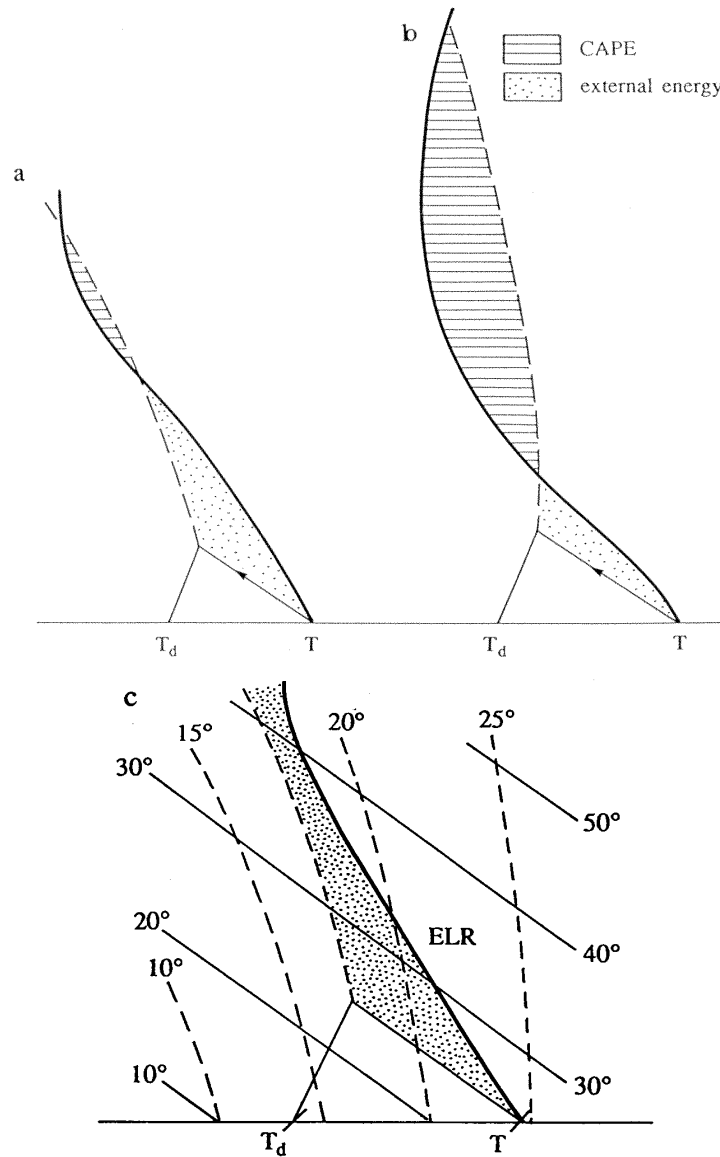

Fig 9.(a-b) soundings with CAPE (i.e. latent instability).(c) a sounding with conditional instability, but without latent instability.

(vi)   Latent instability

The ELR shown on **Fig 9**a is of little concern, whereas a thunderstorm is likely with the ELR on Fig 9b. Notice that not all conditionally unstable soundings display an area of positive buoyancy. A conditionally unstable sounding with, at some level, an area of positive buoyancy (e.g. Fig 9 a-b) is said to have *latent instability*, which is a non-local condition. Conditional instability is a necessary condition for latent instability; the reverse cannot be said, as shown in Fig 9c.

Also notice that point A in Fig 7 does not necessarily correspond with the ground level. Convection normally starts from the level that demands the least amount of external energy. "Elevated convection" is rare in Laramie but quite common in the southeastern US in the spring and fall seasons. In order to evaluate the occurrence and intensity of latent instability in a conditionally unstable sounding, it is useful to construct the *wet-bulb temperature lapse rate* (WLR) from a combination of the ELR and the DLR using Normand's proposition, as shown in **Fig 10**.
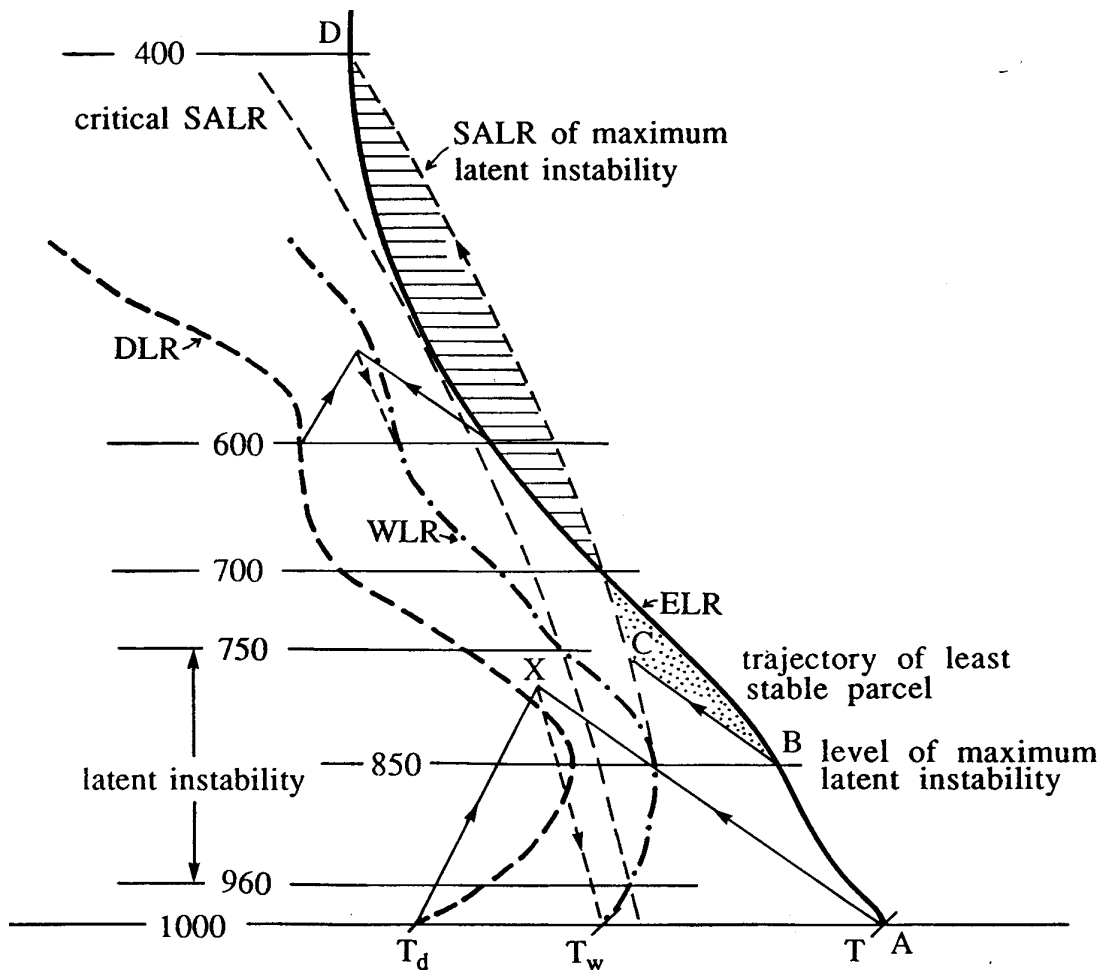
Fig 10. The evaluation of latent instability. Typically the ELR (solid line) and the DLR (dashed line) are based on observations, and the WLR (dash-dot line) is derived at each level, using Normand's proposition. The procedure is shown explicitly at just two levels, 1000 and 600 hPa. The shaded areas show the CIN and CAPE associated with a parcel at the level of highest latent instability, i.e. 850 hPa in this case.

The WLR is useful because all vertical displacements occur strictly along a SALR from any point on the WLR (this follows from the definition of the LCL and Normand's proposition). One can then simply follow a moist adiabat from any point on the WLR, upward, and see whether this moist adiabat intersects with the ELR. If it does, then there is latent instability. In Fig 10, a parcel rising from the ground (line AX) would not intersect the ELR at any level. At 850 hPa however, there is latent instability: a parcel lifted from 850 hPa (line BCD) crosses the ELR and is warmer then the environment between 700 and 400 hPa. Analysis of a series of moist adiabats from the WLR shows

that the sounding has latent instability from level 960 to 750 hPa[2]. This instability is maximum at 850 hPa. Therefore at 850 hPa, any triggering will release the most intense convection. Forecasters will then examine whether there is any indication of possible triggering at that level, e.g. by frontal ascent. Notice that the height of maximum latent instability can change rapidly, and that on warm, sunny days it usually drops to the ground level.
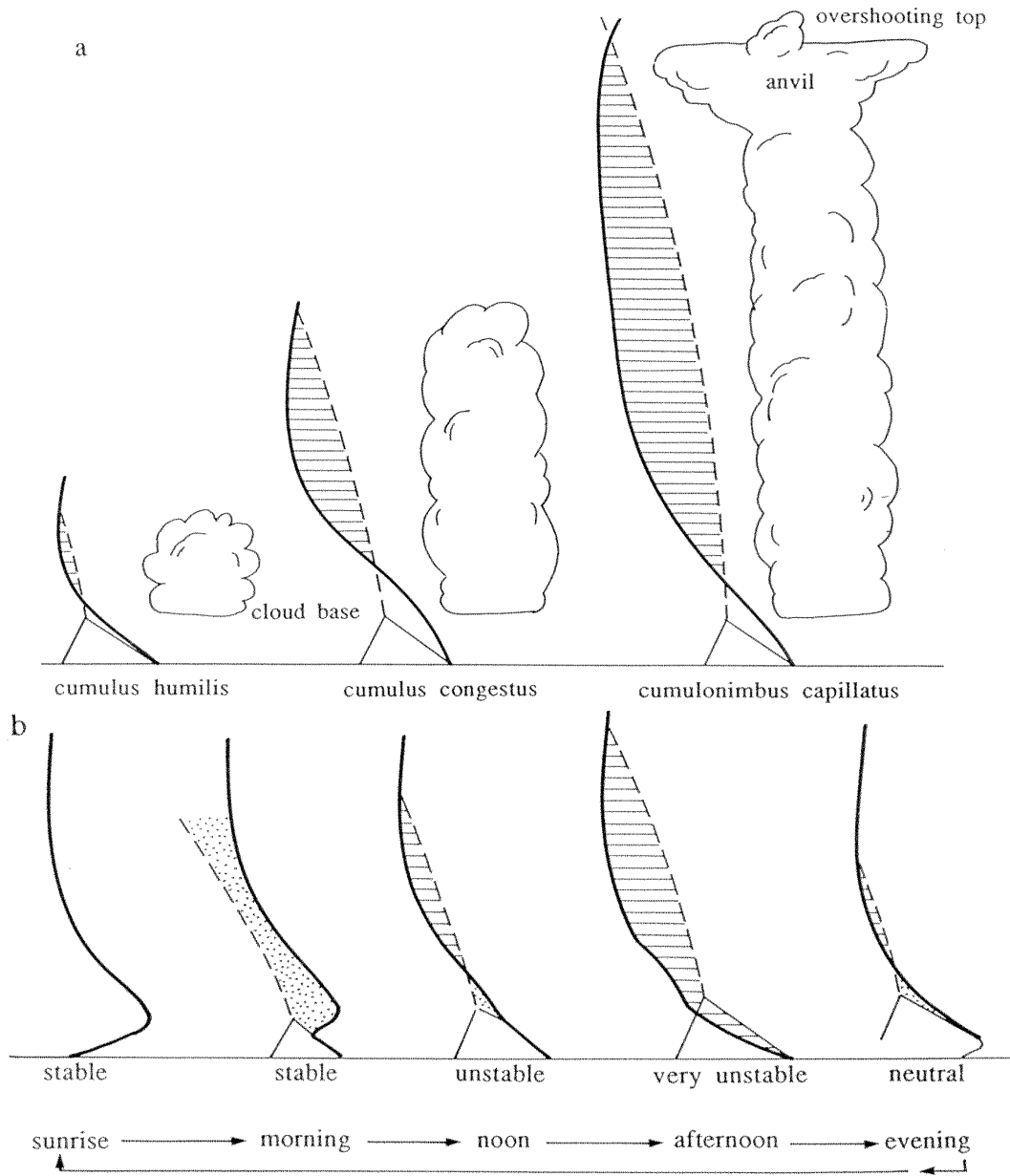
Fig 11. (a) The convective cloud population is trimodal in the tropics (Johnson et al 1999); each type corresponds to different ambient conditions (ELR/DLR). (b) Diurnal cycle of the convective boundary layer, building CAPE, and the more shallow nocturnal radiation inversion. This cycle is obvious in the high Rockies in summer, leading to thunderstorms almost every afternoon.

---

[2] It is a common mistake to claim that the profile has latent instability where the parcel is warmer than the environment, e.g. between 700 and 400 hPa for a parcel starting at 850 hPa. Latent instability is assessed at the parcel's source level, i.e. at 850 hPa.

The amount of CAPE is a function of both the buoyancy of the parcel (or the instability of the ELR) and the vertical depth of the positively buoyant area. Various types of cumulus and cumulonimbus clouds are associated with an increasing vertical depth of the positively buoyant area (**Fig 11**). Providing no change in airmass occurs (i.e. the moisture content remains the same), then morning and early afternoon heating and evening cooling of the PBL will produce a diurnal cycle in the occurrence and depth of convection, with a peak in convective activity in the afternoon (Fig 11b) This cycle is remarkably common over the Rocky-Mountain high terrain in summer. Elsewhere, convective and larger scale dynamics usually alter the phase and the amplitude such a cycle. In any event, CAPE is an important variable for the understanding and forecasting of convection.
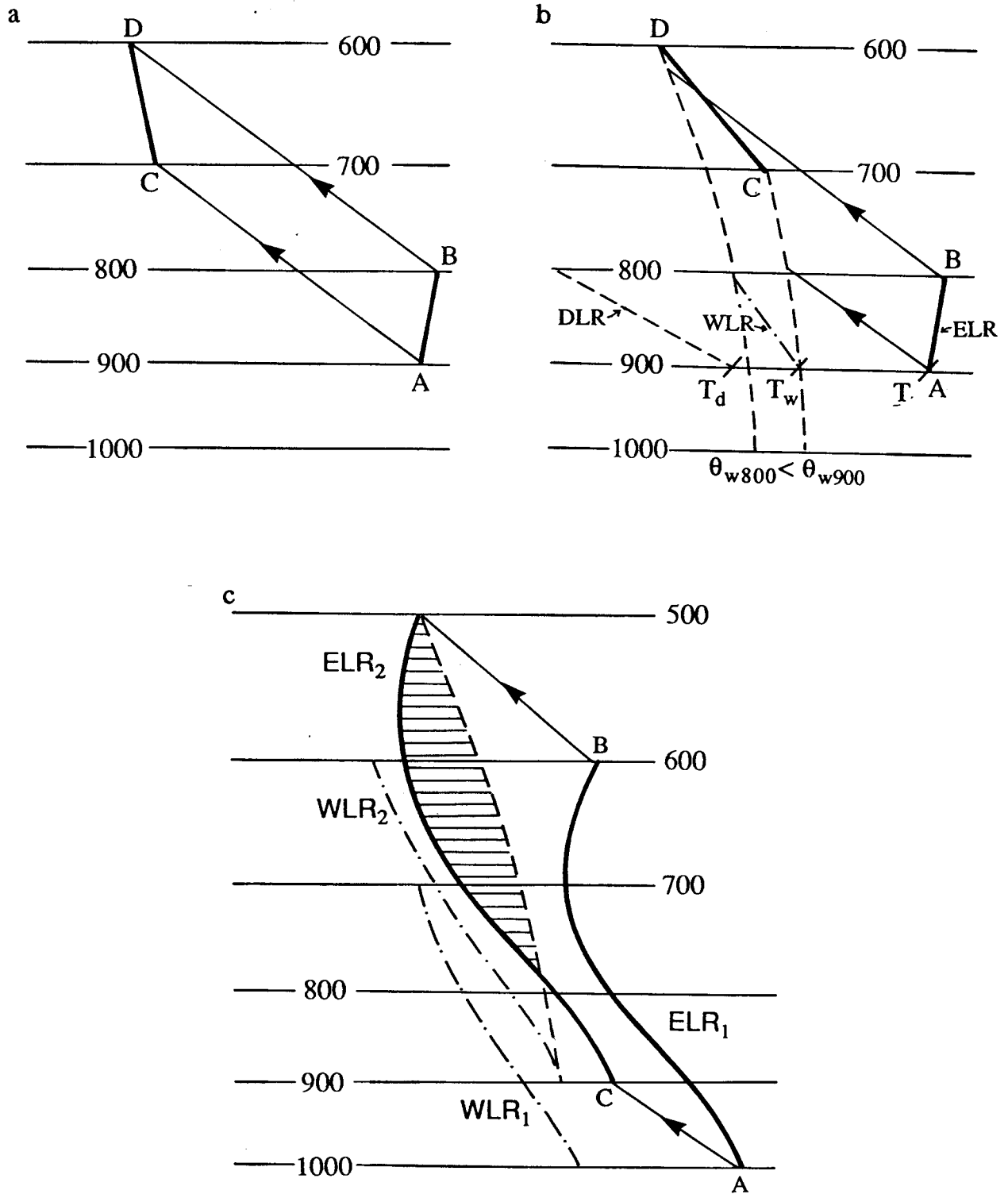
(vii)   Potential instability

So far we have analyzed the stability of a sounding by rising or lowering an air parcel from a certain level and by comparing its temperature with the environment. Now we will examine the effect the lifting of an entire layer has on the stability of that layer. This issue is important because most lifting mechanisms act on a scale much larger then a convective cloud.

In **Fig 12a**, an absolutely stable layer AB is shown between 900 and 800 hPa. This layer is 100 hPa thick, which corresponds to about 1 ton of air per square meter (that follows from the hydrostatic equation). If the air does not diverge in this layer, and typically the divergence is very small, then the layer will still have the same mass when lifted over some distance. Therefore, the layer will still be 100 hPa deep when the bottom is lifted to 700 hPa. We assume that the air is dry enough that no condensation occurs in the lifting. Notice that the layer is now conditionally unstable (Fig 12a, line CD). Clearly, lifting is destabilizing.

Clear destabilization occurs when lifting a layer of air whose lower part is relatively more moist. In Fig 12b, a WLR is derived again from the DLR and the ELR (Normand's principle). You should reiterate at this point that on an aerological diagram at any level a parcel, lifted from the ELR, ascents along a DALR until it intersects with the moist adiabat through the wet-bulb temperature at that level (see Fig 10). Again, we start from an absolutely stable layer AB that is lifted over a depth of 200 hPa. In this case, the lower part of the layer reaches saturation quickly (A to C), whereas the top part ascends dry adiabatically up to just below the 600 hPa level (B to D). At this point, the profile of the layer CD is conditionally unstable, and since it is saturated, the instability is immediate. This is referred to as *potential instability* of the layer AB. The entire layer will now rise along a moist adiabat.

Potential instability is the dominant mechanism of thunderstorm outbreaks, e.g. along a cold front, over a warm front, or near a dryline. It believed to be important also in the case of the widespread fairly heavy rain embedded within lighter rain in extratropical disturbances. Theoretically, the rising will continue until the layer intersects with the ELR. It is not obvious where the ELR is, because the lifting of an entire layer also displaces the layers above. These layers are not necessarily potentially unstable, and therefore, they may resist any further lifting. Therefore, rather than a smooth lifting of the entire potentially unstable layer, one may rather observe small turrets or bands penetrating through the more stable layers aloft. This theory has been used for instance to explain the existence of multiple rainbands (5 to 50 km wide) within a front. In any event, even in the least stable case, the penetration depth of a convectively unstable layer will always be constrained by the tropopause.

The analysis of a set of soundings will show that a simple criterion exists for potential instability: *a layer is potentially unstable when the WLR tilts to the left of the moist adiabats*. Notice that this criterion concerns the slope of the WLR, and not the ELR, as for conditional instability. The criterion is the same as saying that the *wet-bulb potential temperature θ_w decreases with increasing height*. To convince yourself, determine θ_w at various levels on Fig 10. Clearly, θ_w is simply the value of the moist adiabat at any point along the WLR. Now to say that θ_w decreases with height is to say that the moist (potential) energy decreases with height, hence the name potential instability.

Fig 12. (a) Destabilization of a layer of dry air (A-B) by lifting, in this case over 200 hPa; (b) a potentially unstable layer is lifted enough to continue to rise; (c) development of latent instability by large-scale, deep lifting.

Mathematically, the argument is as follows: potential instability occurs when a layer of air, after being lifted to the point where it is saturated, finds itself unstable. That only occurs when that lifted layer of air is conditionally unstable, i.e.

$$\frac{d\bar{\theta}_e^*}{dz} < 0 \tag{6}$$

but the layer of air up there is saturated, so $\theta_e = \theta_e^*$, and also

$$\frac{d\bar{\theta}_e}{dz} < 0$$

Now θ_e is conserved in the case of both dry and saturated adiabatic vertical motion (θ_e^* is only conserved in saturated adiabatic processes). So we can return to the layer's source, where the layer was dry (not saturated), while conserving θ_e, so still:

$$\boxed{\frac{d\bar{\theta}_e}{dz} < 0} \tag{14}$$

This then is the criterion for potential (also called convective) instability (for a layer of air).

Note that $\dfrac{d\theta_e}{dz} = \dfrac{d\theta w}{dz}$, since both θ_e and θ_w can be used to label moist adiabats.

Both conditional and potential instability require external lifting in order to realize the instability. *Conditional instability is conditional to the degree of saturation of the parcel*, and latent instability is conditional to the details of the ELR. *Potential instability occurs when the moist potential energy of a layer decreases with height*.

Fig 12a illustrated that the lifting of a layer may render the air conditionally unstable. Fig 12c shows that even latent instability can be realized by layer lifting. The sounding has some conditional instability at first (AB), but not any latent instability, because the air is too dry. Clearly, lifting of the entire column over 100 hPa (to CD) removes this restriction and makes the sounding rich in CAPE. Strictly speaking, the concept potential instability is used only when lifting renders the layer immediately unstable. But the difference is of little relevance. It is more important to realize that lifting generally destabilizes the environment. This explains in part the orographic enhancement of precipitation: not only does the air rise to cross the mountain crest. Often it rises much more, buoyantly so.

It is also important to realize that any moistening or warming of the lower layers in the troposphere, and any cooling of the upper troposphere, will make vertical instability more likely. Surface heating occurs diurnally; significant changes in stability can occur via differential advection. In the Great Plains, as well as in N. Argentina and Eastern Australia, severe thunderstorms occur typically when low level warm, moist air is advected poleward under an upper level wedge of relatively cold air moving in from the west. The destabilization is enhanced by the presence of sloping terrain (the Great Plains, the Mato Grosso, and the Great Dividing Range), which enhance large scale uplift. Destabilization is occasionally also enhanced by the equatorward penetration of a cold front, which acts like a mountain for the warmer poleward flow.

(viii) Profiles of θ_e, θ_e^*, and CAPE

Typical profiles of θ, θ_e, and θ_e^* were shown in Fig 6. Clearly conditional instability typically occurs over a greater depth than potential instability. **Fig 13** shows the θ_e^* profiles for two tropical regions. From the θ_e^* profile and θ_e at the surface ($\theta_{e,sfc}$), one can obtain the LFC as the level where the $\theta_{e,sfc}$ value intersects the ambient θ_e^* curve. The reason why this intersection is the LFC is that the θ_e of an undiluted parcel rising from the surface is conserved, thus above the LFC, where the parcel is saturated, the parcel θ_e (or moist static energy) is larger than the ambient θ_e^*. On the aerological diagram, the difference between the parcel's moist adiabat (θ_e or θ_w) and the ambient temperature (in terms of moist adiabats on the diagram, this is the ambient θ_e^*) is a measure of the CAPE (J kg^{-1}), at least when integrated vertically from the LFC to the LNB. The latter is the level where $\theta_{e,sfc}$ rejoins the

ambient θ^*_e curve (Fig 8). CAPE can then be calculated (see, e.g., Petersen and Rutledge 2001, Geerts and Dejene 2005) as:

$$CAPE = R \int_{LFC}^{LNB} \left(\theta_{e,sfc} - \theta^*_e \right) d\ln p \tag{15}$$

This expression (15) is a continuous (integral) version of (43). Clearly, on a θ_e–log p graph, *CAPE is proportional to the area* shaded in Fig 13, as is the case on a tephigram. In the Sahel wet season the surface temperature is higher than in the Amazon, but it is drier, thus the LCL and LFC are higher, yet the CAPE is larger. The result is more intense, deeper storms than in the Amazon, but less rain. Amazon thunderstorms are closer to the maritime type, while Sahel thunderstorms are epitomically continental.
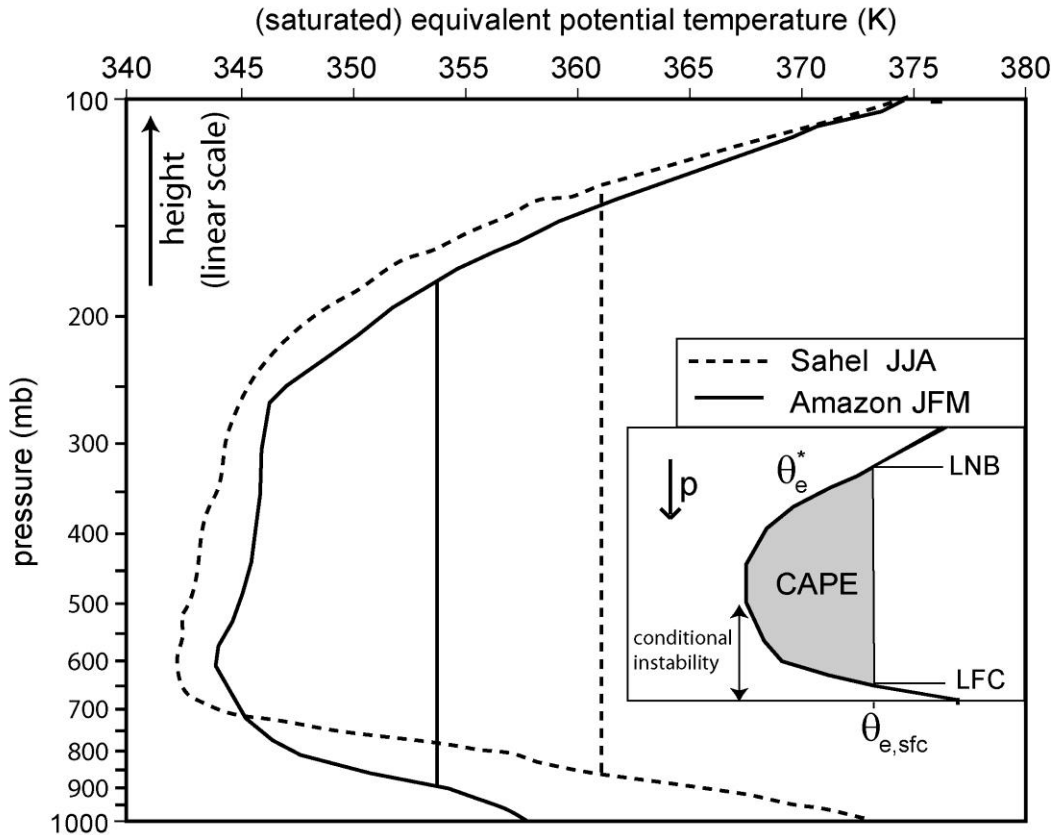
Fig 13. Climatological θ_e^* profiles for the Sahel (Africa) and the central Amazon during their corresponding wet seasons. The profiles are based on the NCAR/NCEP reanalysis dataset.

(ix)   Stability indices

It would be useful to be able to express the degree of instability by a single index. This renders an examination of a large series of atmospheric soundings unnecessary, and allows the mapping. NWP model output or satellite sounder information allows plotting and contouring of that index, which makes a good forecasting tool. Several indices have been developed for this purpose. The names and exact formulae are only given for your further reference, in **Table 2**. They can be grouped in two types:

• **parcel temperature indices**: a parcel is lifted from a prescribed level to another prescribed level, at which its temperature is compared with the environment. The two most common indices used are the lifted index and the Showalter index (Table 2). By definition, the indices have to be negative for any possibility for thunderstorms. For the lifted index, the predicted afternoon maximum temperature at the surface can be used, rather than the observed surface temperature at the time of the sounding (especially if it is in the morning). Or the mean potential temperature

and mixing ratio in the lowest 50-100 hPa can be used to determine the 'best' parcel trace. The value of these indices can be calculated on an aerological diagram, as illustrated in **Fig 14**. Table 2 also lists two modified indices, which involve more parameters. These modified indices may be more reliable, but they involve a calculation rather than simply a graphical estimation on the aerological diagram.

• **fixed-level temperature & dewpoint indices**: these are empirical formulae based on observations of T and T_d at various levels. The parcel technique is not used. The total totals index and the Whiting index are most commonly used. Exactly what values these indices assume when thunderstorm development can be expected is not clear, but a guideline for the critical values is given in Table 1.

index	definition	thunderstorms are possible if	severe thunderstorms are likely if
Lifted index	$LI = T_{500} - T_{pmax}$	LI<0	LI<-8
Showalter index	$SI = T_{500} - T_{p850}$	SI<0	SI<-4
Modified LI	$MLI = LI + (1000 - LCL)/15 + 8$	MLI<0	MLI<-8
Modified SI	$MSI = SI + 0.7(T_{700} - T_{d700}) - 5$	MSI<0	MSI<-4
Total totals index	$TT = T_{850} + T_{d850} - 2T_{500}$	TT>40	TT>55
Whiting index	$WI = T_{850} + T_{d850} + T_{d700} - T_{700} - T_{500}$	WI>15	WI>35

Table 1. Some stability indices. T_{pmax} is the surface daytime maximum temperature, cooled by lifting from the surface to 500 hPa, and T_{p850} is the temperature of a parcel lifted from 850 hPa to 500 hPa. At any pressure level (say 850 hPa), T_{d850} is the dewpoint and T the (dry bulb) temperature. LCL is the lifting condensation level (in hPa). All temperatures are expressed in °C or K.
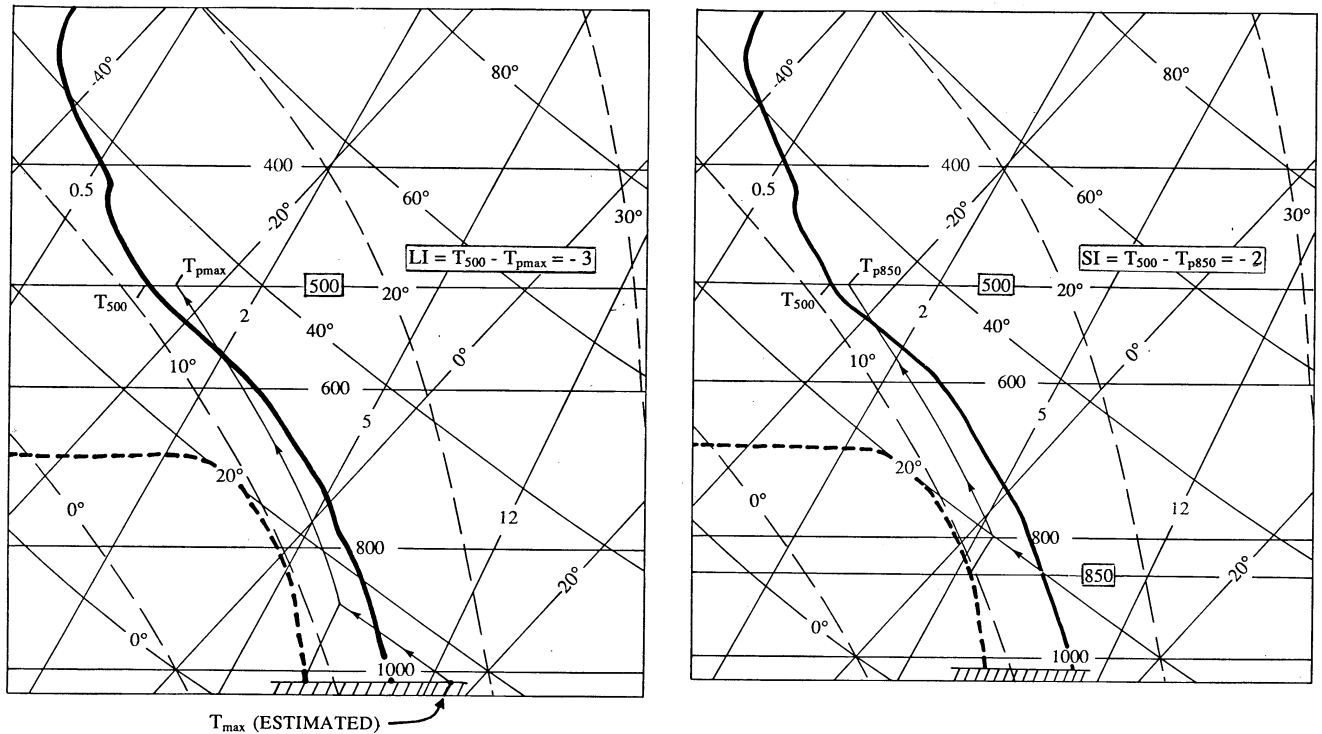
Fig 14. The calculation of the lifted index (LI), left, and the Showalter index (SI), right.

References

Geerts, B. and T. Dejene, 2005: Regional and diurnal variability of the vertical structure of precipitation systems in Africa, based on spaceborne radar data. *J. Climate*, **18**, 893-916.

Johnson, R. H., T. M. Rickenbach, S. A. Rutledge, P. E. Ciesielski, and W. H. Schubert, 1999: Trimodal characteristics of tropical convection. *J. Climate.,* **12**, 2397–2418.

Manual of Meteorology, 1975: Australian Bureau of Meteorology, Rev. Ed. Pt. 1, General Meteorology, QC864-A8/1975.

Petersen, W. A., and S. A. Rutledge, 2001: Regional variability in tropical convection: Observations from TRMM. *J. Climate*, **14**, 3566-3586.

Preston-Whyte and Tyson, 1988: *The Atmosphere and Weather of Southern Africa*. Oxford University Press, 375 pp. QC991.Al.P74.

Stull, R.B. 1991: Static Stability - an update. *Bull. Amer. Meteor. Soc.*,**72**, 1521-1529